Available online at www.sciencedirect.com

ScienceDirect

Procedia Engineering 101 (2015) 101 – 108

Procedia Engineering

www.elsevier.com/locate/procedia

3rd International Conference on Material and Component Performance under Variable Amplitude Loading, VAL2015

Fatigue behavior of stiffener to cross beam joints in orthotropic steel decks

Pietro Croce[a,*], Daniele Pellegrini[b]

[a] *Dipartment of Civil and Industrial Engineering - DICI, University of Pisa, Largo Lucio Lazzarino, Pisa 56122, Italy*
[b] *Institute of Information Science and Technology "A.Faedo" - ISTI, Italian National Research Council (CNR), via G. Moruzzi 1, Pisa 56124, Italy*

Abstract

In the paper the possibility to evaluate the fatigue strength of stiffener to cross beam joints in orthotropic steel decks is discussed. The proposed methodology, based on Paris-Erdogan law, allows to derive a sound estimate of the stress intensity factor K combining the indirect approach, based on the Rice J-integral, with the direct one, based on the extrapolation of experimental or numerical data. The practical implementation of the proposed methodology allowed to predict correctly the actual fatigue life of a previously tested real scale specimen, so validating its potentialities.

Peer-review under responsibility of the Czech Society for Mechanics

Keywords: orthotropic steel bridge decks; fatigue; stiffener to cross beams joints; cope hole; J-integral; stress intensity factor.

1. Introduction

Orthotropic steel decks are widely used in medium and long span bridges, where the control of the self-weight of the bridge is crucial even for the feasibility of the bridge itself.

As known, typical welded details of orthotropic decks, stiffeners to deck plate joints, stiffener to stiffener joint and stiffener to transverse beam joints are particularly sensitive to fatigue. In fact fatigue cracks have been detected during the last decades in several orthotropic steel bridge decks around the world, after just ten or twenty years of

* Corresponding author. Tel.: +39-050-2218206; fax: +39-050-2218201.
E-mail address: p.croce@ing.unipi.it

Peer-review under responsibility of the Czech Society for Mechanics
doi:10.1016/j.proeng.2015.02.014

service life [1]. The risk of fatigue cracks is further amplified considering that, in the second half of the 20th century, the aggressiveness of the road traffic, both in terms of vehicle flow and axle and vehicle weighs, increased, together with the structural performance demand. Nevertheless, while the knowledge about the fatigue behavior of stiffeners to deck plate joints and stiffener to stiffener joints has been deeply improved by recent studies, the fatigue behavior of stiffeners to transverse beam joints is still open, because it strongly depends on the complexity of the stress pattern and on the local stress peaks [1], [2].

A specific research work, motivated by the observation of fatigues cracks detected in welded joints in European orthotropic steel bridges, is discussed, paying particular attention to stiffeners to transverse beam joints with cope hole, also considering the results of original experimental fatigue tests on true scale specimens [3], [4], [5].

In stiffeners to crossbeam joints with cope hole, fatigue cracks usually occur in the web of the transverse beam at the free edge of the cut-out, sometimes propagating in the stiffeners, while, in other cases, longitudinal fatigue cracks happen in the web of the stiffeners. These longitudinal cracks start in the stiffener, at the toe of the welding connecting the transverse beam with the stiffener itself, and sometimes they propagate even in the web of the crossbeam. In the area of locations where fatigue cracks are expected, the stress patterns and the stress concentrations strongly depend on local geometry of the detail and on the presence and shape of cope holes, so that the fatigue behavior of these details cannot be directly predicted using the standard fatigue classifications and the associated *S*-*N* curves, which are generally plotted in terms of nominal stresses, disregarding stress peaks. For these reasons, the fatigue classification of stiffener to transverse beam joints requires extensive fatigue tests campaign on real scale specimens. Due to the influence of local geometry on the stress concentration, the fatigue classification and the *S*-*N* curves should be derived in terms of peak stresses, so that, despite of the considerable costs of the tests, experimental results are valid only for the individual joint typology under investigation and their significance cannot be easily extended. In this respect, the setup of numerical procedures founded on fracture mechanics laws could allow to widen considerably the field of application of the available experimental results.

The evaluation of the fatigue strength of these details is discussed and illustrated in §2, while the practical application of method, based on fracture mechanics laws, is described in §4, referring to a significant case study.

2. Fatigue models.

Describing fatigue phenomenon, it is usual to distinguish, depending on the level of stress, on the extension of the plastic zone and on the number of cycle to failure, true fatigue from low-cycle fatigue.

The phenomenon is identified as (true) fatigue when the plasticized zones are concentrated in the vicinity of the stress concentrators or at the apex of the cracks and their extension is very small if compared with the typical dimensions of the detail. The nominal stresses, that are those obtained disregarding the stress concentrations, are in the elastic field and, therefore, the number of cycles to failure is high, for example $N>10^4–10^5$.

On the contrary, when dimensions of plasticized zone are comparable with the typical dimensions of the detail, the number of cycles to failure is low and the phenomenon is identified as low-cycle fatigue.

The present paper refers only to true fatigue.

Since *S*-*N* curves are deduced with the assumptions of constant amplitude load cycles, appropriate damage calculation criteria should be introduced to extend the validity of the *S*-*N* curves themselves also in case of varying amplitude stress histories. The damage criteria commonly adopted in fatigue strength assessment of steel details is the Palmgren-Miner's damage accumulation law [6], [7], which considers the damage as *time independent* and *interaction-free*; time independency hypothesizes that the damage produced by one stress cycle is the same whichever the time *t* of its occurrence, while, in addition, lack of interaction, assumes that the damage produced by one stress cycle is independent on previously accumulated damage, so that fatigue damage results linearly additive.

More recently several studies have been addressed to very intricate aspects, regarding not only the deepening of the knowledge and the refinement of the assessment procedure, but also the philosophy and the conceptual background of designing against fatigue, so that concepts used in other engineering branches, like *damage tolerant design* or *reliability analysis*, are becoming widely accepted.

The method discussed here after aims to derive an alternative procedure to assess the structural fatigue strength, starting from the crack propagation laws adopted in fracture mechanics theory [3], [10].

Said a the crack length and N the number of cycles, the crack propagation rate da/dN under constant amplitude stress histories can be generally expressed by

$$\frac{da}{dN} = C(Y(a)\Delta\sigma_a\sqrt{\pi a})^m , \quad (1)$$

where σ is a representative value of the stress level and C a material constant.

Generally, the crack propagation rate da/dN is a function of the stress intensity factor range ΔK, which is the variation of the stress intensity factor in the stress cycle. The stresses at the crack tip for the three basic crack propagation cases, *n=I (opening)*, *II (in-plane shear)*, *III (out-of-plane shear)* can be expressed by

$$K_j = Y_j\,\sigma_a\sqrt{\pi\,a}\,, \quad (2)$$

where K_j represents the stress intensity factors pertaining to the basic propagation mode, j is the basic case number, Y_j is the geometry factor and σ_a is the nominal stress, derived from a detailed description of the stress system in the vicinity of the crack (but not influenced by it). Analogously, in the three basic cases ΔK_j can be expressed by

$$\Delta K_j = Y_j\,\Delta\sigma_a\sqrt{\pi\,a}\,, \quad (3)$$

so that ΔK_j depends on the applied loads, on the crack geometry and on the geometry of the element.

Since the values of ΔK_j can be determined from the path-independent Rice integral, J, [9] or directly, two alternative methods are proposed here to obtain them effectively through refined finite element analysis.

The first method is based on the application of Rice theory: in 2-D linear fracture mechanics, the energy release rate J for growth of a crack lying on x_1 direction is equal to the value of the 2-D J-integral, given by

$$J = \int_{\Gamma}\left(W(x_1, x_2)\,dx_2 - T_i\frac{\partial u_i}{\partial x_1}ds \right), \quad (4)$$

where W is the density of the strain energy, Γ is an arbitrary path clockwise around the apex of the crack, u_i the components of the displacement vectors, $T_i=\sigma_{ij}\,n_j$ are the components of the surface traction vector $\boldsymbol{T}$, being $\boldsymbol{n}$ the outward normal to Γ, and ds an incremental length along the path Γ. The J-integral is zero if calculated along a closed path, while it is constant along any path that starts and ends at the edges of the crack. Irwin showed that for crack opening mode I, G and therefore J-integral, is related to stress intensity factor K_I by the following expressions:

$$G = J = \begin{cases} \dfrac{K_I}{E} \\ \dfrac{(1-\nu^2)K_I}{E} \end{cases}, \quad (5)$$

where E is the Young's modulus and ν is Poisson's modulus; the first equality holds in the plane stress case, the other one in the plane strain case.

The stress intensity factor can be so trivially derived from equation (5), provided that the J-integral value is known. In practice, the J value can be determined via FEM analysis using suitable finite element software, but doing so it loses its fundamental characteristic, the path independence: in effects, its value depends on the mesh accuracy, in other words on the mesh refinement and in mesh orientation, as well as on criteria adopted for choosing of the computation path.

To reduce the uncertainties inherent with the finite element evaluation of J value, it is possible to proceed in an alternative way, directly calculating the stress intensity factor K_J from equation (2), also in view to combine the two approaches.

Assuming that the angle with respect to the plane of the crack is zero and recalling that the stress field around the crack tip is given by:

$$\sigma_p = \frac{K_I}{\sqrt{2\pi\, r_i}}, \tag{6}$$

where σ_p is the Cauchy stress valuated in a generic point P at a distance r_i from the crack tip itself, it is possible to derive the geometric factor Y_j,

$$Y_j = \frac{\sqrt{2\, r_i}}{\sqrt{a}} \frac{\sigma_p}{\sigma_a}, \tag{7}$$

combining expressions (2) and (6).

Regardless the stress intensity factor is calculated using equation (5) or equation (7); to evaluate the number of cycle to failure it is necessary to adopt a suitable expression for the crack propagation law, like the widely used Paris-Erdogan law [8],

$$\frac{da}{dN} = C\left(\Delta K^m\right), \tag{8}$$

adopted in the following. In equation (8), C and m are material constants, which can be determined, for example, from experiments on simple specimens.

Substituting (2) in (8), it results

$$\frac{da}{dN} = C\left(Y(a)\Delta\sigma_a\sqrt{\pi\, a}\right)^m, \tag{9}$$

from the integration of which, it is possible to derive, for a given detail and an initial crack of size a_0, the number of cycles that the detail can carry till to unstable propagation of the crack and complete failure of the detail itself:

$$N = \int_0^N dN = \int_{a_0}^{a} \frac{da}{C\left(Y(a)\Delta\sigma_a\sqrt{\pi\, a}\right)^m}, \tag{10}$$

where a is the critical crack length.

A practical application of methods described above, is shown in §4.

3. Experimental tests

The study of fatigue behavior of stiffeners to crossbeam joints with cope hole is an active field of research at Structural Section of Department of Civil and Industrial Engineering (DICI), even in the framework of wide research programs promoted by the European Community [4], [5]. In order to know full well this problem, analytical and numerical calculations should be supported by experimental tests. To this end at DICI's laboratory were performed a large number of static and fatigue tests on real scale specimens.

Static tests, complemented by finite element numerical analyses, were aimed to identify the optimal shape of the cut out, since a change in itself can determine even modification of the failure modes. By these analyses it has been deduced the need to employ rigid transverse beams and to make cut-out having very large curvature radius of the free

edge. Exploiting these information, two different joints have been made for the implementation of fatigue tests: the first, indicated as specimen A (see Fig.1.a), having a classic circular cope hole, in case of triangular stiffeners; the second, specimen B, having an innovative wide-radius cope hole (see Fig.1.b). The fatigue tests were carried out applying two fatigue loads $P/2$ at the ends of the stiffeners, symmetrically with respect to the transverse beam web plane, between two stiffeners, according to the fatigue test arrangement shown in Fig. 2: the figure refers to specimen A, but a similar scheme was adopted for the specimen B too. The fatigue tests were performed with constant amplitude pulsating loads with a frequency of 1,8 Hz about: each cycle was characterized by P_{max}=244 kN, while a small non-zero value P_{mis}=14 kN was adopted for practical reasons, to avoid shaking of the specimen itself.

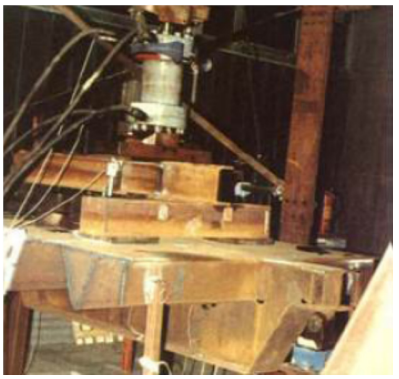

Fig.1. (a) Specimen A

Fig.1. (b) Specimen B

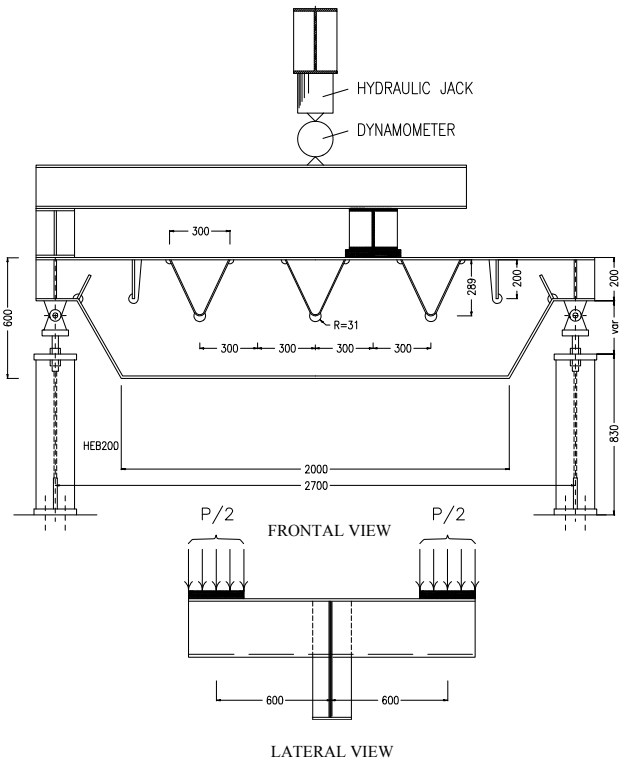

Fig.2. Fatigue test arrangement for specimen A

Fatigue tests carried out on specimens described above, confirm that fatigue crack usually occurs in the web of the transverse beam, at the free edge of the cut-out, sometimes propagating in the stiffeners (Figs. 3.a and 3.b). In other cases, longitudinal cracks appear in the web of the stiffeners (fatigue crack 2 in Fig. 3.b), at the end of the welding with the web of the transverse beam, due to residual stresses and out-of-plane bending of the stiffener web. Tests show that unstable propagation of the crack occurs around $5 \cdot 10^5$– $6 \cdot 10^5$ cycles, when the crack length a is 60 mm about, determining the joint failure.

4. Practical application of the proposed method

To validate them, the methods proposed in §2 [3] have been applied to the real scale specimens tested in fatigue and described in §3, aiming to reproduce the experimental fatigue behavior. The stress intensity factors have been determined directly or by means of the J-integral through very refined finite element analyses: for instance, the finite element models representing specimen B is represented in figure 4.

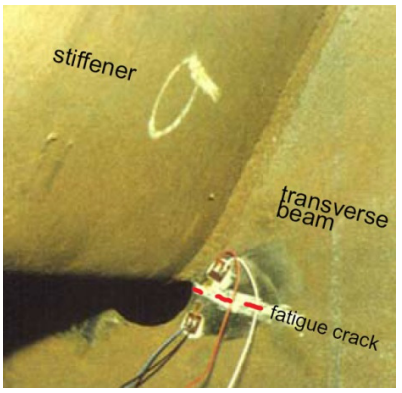

Fig. 3. (a) Fatigue crack - Specimen A

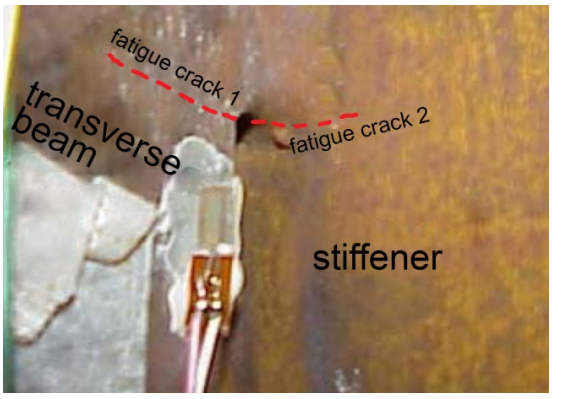

Fig. 3. (b) Fatigue cracks - Specimen B

Each model has undergone a linear elastic analysis, considering an applied static load equal to the maximum value of the cyclic load applied to the specimens in each fatigue test, inserting cracks of initial length a_0, and increasing length a at the free edge of the cope hole: the analysis was stopped when a=60 mm, according to experimental evidence. In figures 5.a and 5.b finite element details in the crack zone are shown for specimens A and B, respectively, while in figure 5.c the crack of specimen A is further emphasized.

The minimum principal stress has been then evaluated in the vicinity of the apex of the cracks, as a function of the distance r_i from the crack tip, in such a way to determine the peak stress. Solid curves in figures 6.a and 6.b show the σ–r_i curves corresponding to different crack length a for specimens A and B, respectively, while dashed lines show the corresponding nominal stress trends, obtained by linear extrapolation of the data to the crack apex. Curves Y–r_i are finally displayed in figures 7.a and 7.b. The knowledge of peak stresses and nominal stresses at the crack apex allows so to evaluate ΔK_j, starting from (7), or alternatively by the first of (5). In the crack propagation simulation, only mode I is considered, disregarding crack closure effect, as no reversal of load occurs, while stress intensity factor is derived from the J-integral in plane stress condition.

Tables 1 and 2 show the results of the two numerical procedures, in terms of stress intensity factors $K_{I,Y}$ and $K_{I,R}$, calculated by geometrical factor Y and J-integral, respectively. Finally, figure 8 shows the K-$a^{1/2}$ curves, calculated via "Y-method" and via "J-method" for model A, together with the interpolating exponential regression lines. Placing one of these regression laws in eq. (8), and integrating it, a can be obtained as a function of N, thereby determining the number of cycles to failure or the crack critical length, corresponding to crack unstable propagation.

The results of such elaborations are illustrated in figure 9, where the green curve refers to direct evaluation of K, while the red one refers to J-integral; it can be observed that the predicted number of cycle to failure is about $5{\cdot}10^5$ via J-integral and around $6.1{\cdot}10^5$ by direct estimation of K, in good agreement with the experimental results recalled in §3 ($5{\cdot}10^5$– $6{\cdot}10^5$ cycles to failure).

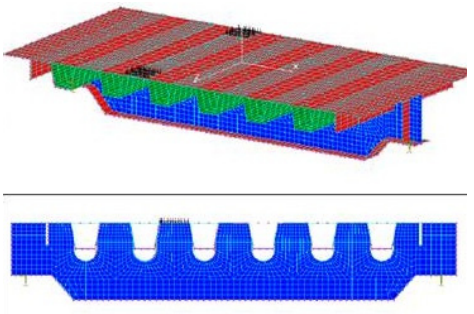

Fig. 4. Finite element model - Specimen B

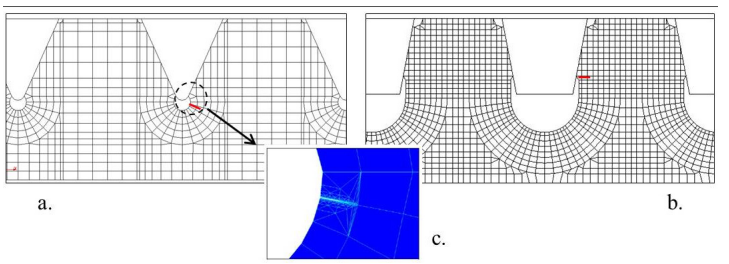

Fig.5. Crack detail: (a) Specimen A; (b) Specimen B; (c) Zoom of cope-hole of specimen A

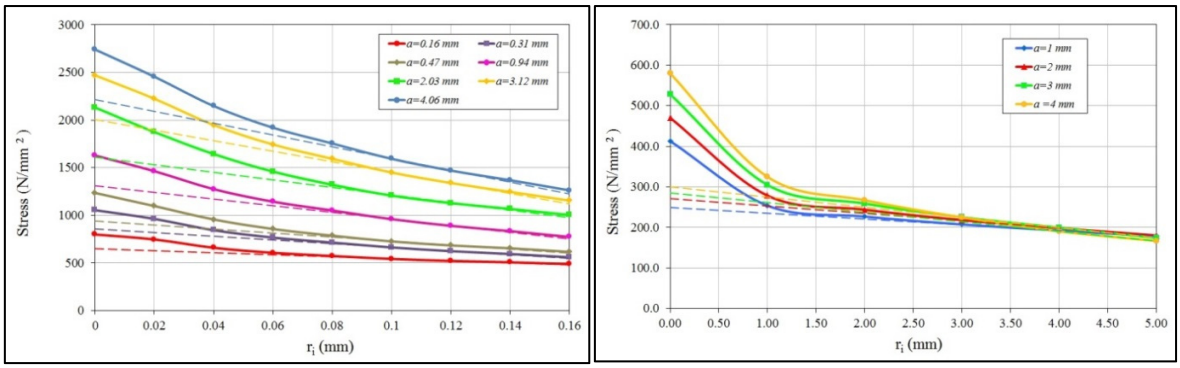

Fig.6. Minimum principal stress field (a) Model A; (b) Model B

Table 1. Results of Model A analysis.

a (mm)	σ_p (N/mm^2)	σ_{nom} (N/mm^2)	Y	$K_{I,Y}$ $(N/mm^{3/2})$	$K_{I,R}$ $(N/mm^{3/2})$	$\Delta\%=\lvert K_{I,Y}-K_{I,R}\rvert/K_{I,R}$
0.16	799.8	650.3	0.586	270.35	258.94	4.5%
0.31	1055.1	858.4	0.418	354.51	379.26	6.5%
0.47	1236.0	941.4	0.344	393.89	418.76	5.9%
0.94	1628.6	1311.4	0.242	546.48	604.90	10.7%
2.03	2132.9	1610.7	0.168	684.57	832.57	17.8%
3.12	2470.0	2005.7	0.134	843.82	912.50	7.5%
4.06	2740.9	2215.4	0.117	925.92	--	--

Table 2. Results of Model B analysis.

a (mm)	σ_p (N/mm^2)	σ_{nom} (N/mm^2)	Y	$K_{I,Y}$ $(N/mm^{3/2})$	$K_{I,R}$ $(N/mm^{3/2})$	$\Delta\%=\lvert K_{I,Y}-K_{I,R}\rvert/K_{I,R}$
1.0	413.2	249.3	1.493	659.77	617.08	6.9%
2.0	470.3	271.2	1.056	717.69	707.38	1.4%
3.0	528.5	300.2	0.862	794.31	808.45	1.7%
4.0	580.1	285.1	0.843	851.96	895.73	4.9%

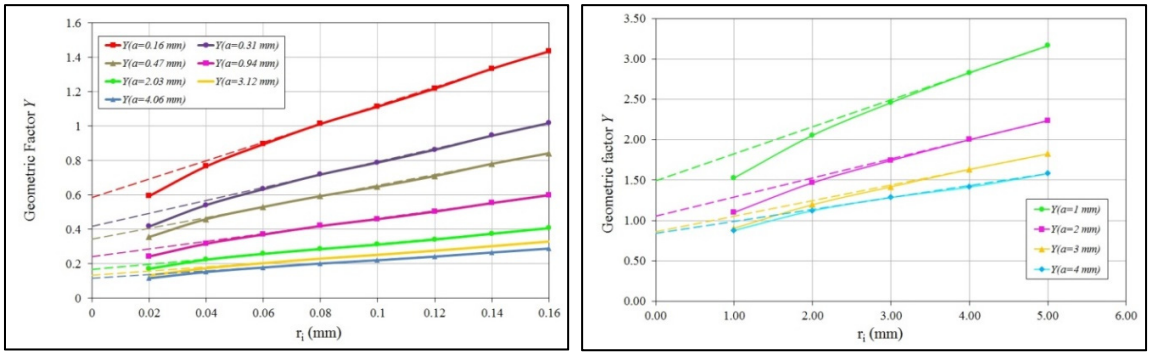

Fig.7. *Y* geometric factor trend (a) Model A; (b) Model B

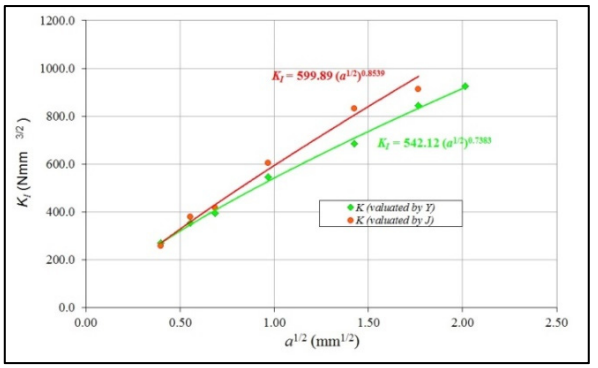

Fig.8. Model A: $K - a^{1/2}$ curves

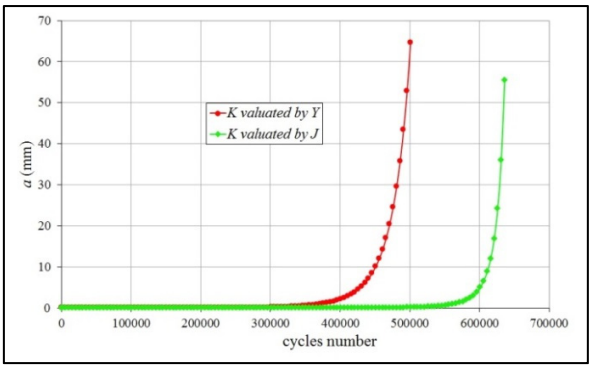

Fig.9. Model A: $a - N$ curves

5. Conclusions

Two numerical procedures to determine, via finite element analysis, the stress intensity factor K to be used in Paris-Erdogan law, have been illustrated. In the first method, the stress intensity factor K is derived from the Rice J-integral, while in the second method K is directly determined through the extrapolation of numerical or experimental data at the apex of the crack. The combination of the two methods allows to perform a cross check of the results, in such a way that uncertainties are reduced and the estimation of K is improved.

Finally, the proposed methods have also been applied to real scale specimens of stiffener to transverse beam joints, previously tested in fatigue. The results confirm that the predicted number of cycles to failure is in good agreement with the test results, so validating the methods; anyhow, additional studies are in progress, aiming to explore the full potential of the methods themselves.

References

[1] De Jong F.B.P., Renovation techniques for fatigue cracked orthotropic steel bridge decks, Faculty of Civil Engineering and Geosciences, 2007

[2] Kolstein M.H., Fatigue Classification of Welded Joints in Orthotropic Steel Bridge Decks, Dissertion, Faculty of Civil Engineering and Geosciences, 2007

[3] Pellegrini D., Rotture per fatica nei giunti saldati di impalcati da ponte a piastra ortotropa, PhD thesis, PhD Course Science and Technology of Civil Engineering, Pisa, 2009/2010, supervisor P.Croce

[4] Croce P., Sanpaolesi L., Rehabilitation of fatigue damaged orthotropic steel deck bridges, Proceeding of International Conference on Bridge Maintenance Safety and Management IABMAS'02 (2002)

[5] Caramelli S., Croce P., Froli M., Sanpaolesi L., Misure e interpretazioni dei carichi dinamici sui ponti-quarta fase: resistenza a fatica dei ponti in acciaio, Final Technical Report CECA N0 7210-SA/415, University of Pisa (1994)

[6] Palmgren, A. Die Lebensdauer von Kugellagern, Z. Vereins Deutscher Ingenieure; Vol. 68: 339-341, 1924

[7] Miner, M.A., Cumulative damage in fatigue, Journal of Applied Mechanics, Vol. 12: pA159-A164, 1945

[8] Paris, P. C., Erdogan F., A critical analysis of crack propagation laws, Journal of Basic Engineering, Vol. 85D, pp. 528-534, 1963.

[9] Rice, J. R., A path independent integral and the approximate analysis of strain concentration by notches and cracks, Journal of Applied Mechanics, 35: 379–386, 1968.

[10] Kornél K., Làszlò D., Fracture mechanics based fatigue analysis of steel bridge decks by two-level cracked models, Computer & Structures, Volume 80, Issue 27-30, pp. 2321-2331, November 2002